PCCP

Accepted Manuscript

This is an *Accepted Manuscript*, which has been through the Royal Society of Chemistry peer review process and has been accepted for publication.

Accepted Manuscripts are published online shortly after acceptance, before technical editing, formatting and proof reading. Using this free service, authors can make their results available to the community, in citable form, before we publish the edited article. We will replace this *Accepted Manuscript* with the edited and formatted *Advance Article* as soon as it is available.

You can find more information about *Accepted Manuscripts* in the Information for Authors.

Please note that technical editing may introduce minor changes to the text and/or graphics, which may alter content. The journal's standard Terms & Conditions and the Ethical guidelines still apply. In no event shall the Royal Society of Chemistry be held responsible for any errors or omissions in this *Accepted Manuscript* or any consequences arising from the use of any information it contains.

ROYAL SOCIETY OF CHEMISTRY

www.rsc.org/pccp

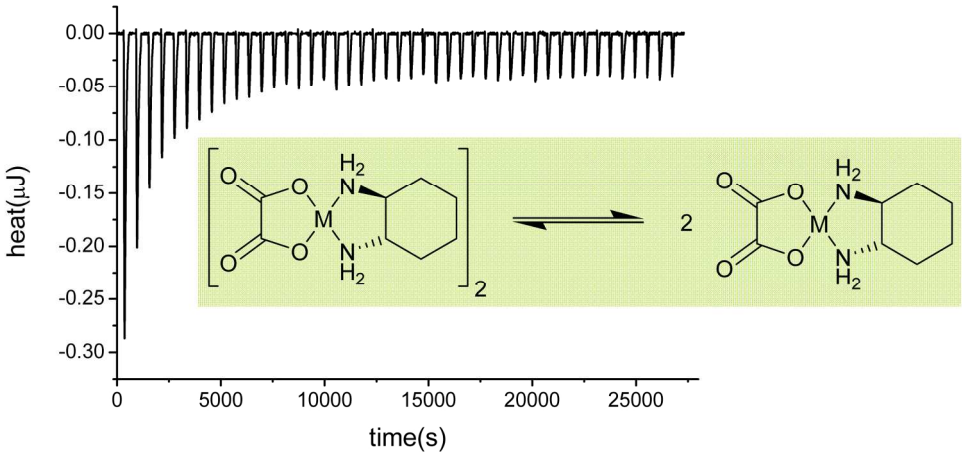

The issue of self-aggregation of Oxaliplatin in water as well as in the gas phase is investigated analytically and analyzed by state-of-the-art DFT-D methods.
178x87mm (300 x 300 DPI)

Physical Chemistry Chemical Physics

Dynamic Article Links ►

Cite this: DOI: xxx

Article

www.rsc.org/xxxxxx

Experimental and theoretical investigations on the self-association of Oxaliplatin.

Predrag V. Petrović,[a,b] Stefan Grimme*[c], Snežana D. Zarić*[b,d], Michel Pfeffer[a] and Jean-Pierre Djukic*[a]

Received (in XXX, XXX) Xth XXXXXXXXX 20XX, Accepted Xth XXXXXXXXX 20XX
DOI: 10.1039/b000000x

Self-aggregation in water of anti-cancer agents such as Oxaliplatin (**1**) or its palladium-containing parent (**2**) is suspected to be the main reason for the exceptional resistance of concentrated infusions of these complexes to hydrolysis; this hypothesis, i.e the self-association of metal chelates, was investigated in a systematic manner by experimental and theoretical means. ^{1}H diffusion-ordered NMR spectroscopy (DOSY NMR) and UV-visible absorption titration were inconclusive as to the formation of a dimer of **1** in water or DMSO. Further isothermal titration calorimetry (ITC) methods allowed the accurate determination of the enthalpy of formation of only the homodimer [**2**]$_2$ and putative heterodimer [**1•2**] together with an estimation of the formation constants, which indicate that dimer formation is not a spontaneous process in solution, whereas electrospray ESI mass spectroscopy tends to suggest the contrary in the gas phase. A dispersion-corrected DFT method, i.e DFT-D (BLYP-D3), was used to model the aggregation in solution (COSMO) and to investigate the assisting role of London force in the cohesion of bimolecular aggregates. The concordance of experimental and theoretical thermodynamic parameters was judged reasonable even though the treatment of solvation by conventional continuum models does not account for specific interactions of the solute with molecules of solvent; nonetheless these results outline the importance of dispersion, a.k.a. London force. The role of the latter was further stressed by computing the affinities of **1** and **2** for the lipophilic cavity of cucurbit[7]uril in modeled water (COSMO-RS), which were preliminarily determined experimentally by ITC methods using pure water as solvent. From our investigations carried out in pure water the connection between the notorious chemical stability of "concentrated" infusions of **1** in aqueous media and the formation of oligomers remains unsettled.

1. Introduction

The discovery of the cytotoxicity of Cisplatin[1] in the mid 1960's has opened a new paradigm for transition metal chemistry, that is the use of coordination complexes for the therapeutic treatment of diseases such as cancers. Clinical limitations imparted to the toxicity of Cisplatin motivated the development of new anti-cancer agents by borrowing to Cisplatin the cis-bisamminoplatinum(II)$^{2+}$ motive, considered essential to preserve cytotoxic properties, which stem from the Cisplatin-induced deformation and denaturation of tumor DNA.[2,3] Oxaliplatin (Eloxatin™) and Carboplatin belong to this class of clinically approved drugs that display a different spectrum of activity on various lineages of malign cells[2,4] and also show a whole range of new side effects[5] that dictate cautious formulations.[6] In a recent report, Dabrowiak et al.[7] raised the issue of the unusual shelf stability of concentrated infusions of Carboplatin and Oxaliplatin and proposed, basing their conclusions on NMR spectroscopic analyses, that these complexes exist as dimers in relatively concentrated solution, which would explain why their hydrolysis to bis aquo complexes,[8-10] a likely process in dilute neutral and basic aqueous preparations,[11] is apparently precluded in concentrated infusions. This proposal was supported by striking spectroscopic evidence of oligomer formation in the gas phase thanks to ESI mass spectroscopy.[7] Such behaviour in solution and in the gas phase was already known[12] for other Cisplatin-type structures but never investigated before Dabrowiak's paper. Nonetheless, the question of the nature of the forces driving these complexes to form oligomers of sufficient persistence in solution or in the gas phase remained open. It is evident from a scrutiny of available crystallographic information that the solid state structuration of these Cisplatin-type complexes is governed by the directing effect of intermolecular H-bonding, favoring various modes of intermolecular arrangements (stacks, strands).[13, 14] However, a simple observation of supramolecular networks does not tell much about the likely behaviour of these molecules in molecular assemblies of smaller scale in gas phase or solution wherein dispersion forces, i.e the often overlooked London forces, combined to H-bonding may play a key role in ensuring the cohesion of a putative "non-covalent dimer" of different structure. This issue of the spontaneous agregation of square planar d^{10} platinum complexes raises also the question of the real weight of correlation-based intermetallic *d-d* interactions[15-17] in the overall cohesion of the aggregates that was addressed by our group recently.[18] In this article, we provide an extensive report on the study of the dimerization of therapeutically important anti-cancer drug Oxaliplatin by a combination of experimental and theoretical investigations carried out with state-of-the-art methods. We also provide a new insight on the theoretical treatment of non-covalent interactions by DFT-D under the challenging conditions of solvation.

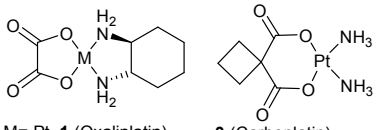

Figure 1. Pt(II) and Pd(II) coordination complexes considered in this report.

2. Results and discussion

The core of Dabrowiak's findings is based on the ^{1}H NMR investigations of water solutions of either Carboplatin or Oxaliplatin buffered with HEPES (4-(2-hydroxyethyl)-1-piperazineethanesulfonic acid). Whereas these conditions probably reproduce physiological conditions in term of *pH*, the use of a potential chelating Lewis base such as HEPES raised our concern about the well documented interactions of this piperazine-based buffer with the considered class of platinum complexes,[19,20] which could question the reliability of the NMR signal assignment provided by Dabrowiak. For the sake of clarity, we opted for a different methodology that privileged the use of pure polar solvents of high dielectric constants and of either protic (D_2O) or aprotic nature (d_6-dimethylsulfoxide); the aim being to restrict to a minimum the interferences from unwanted processes such as ligand exchange and disruption of chelation. We show farther that another buffer such as TRIS (tris(hydroxymethyl)aminomethane), which is also a potential ligand of Pt(II),[19,20] is far from being innocent when reliable evaluation of the energetics of non-covalent interactions is at stake. For the purpose of comparison, all experiments carried out with Oxaliplatin **1** were also carried out with its palladium-containing analogue **2**,[21] a complex known for being nearly exempt of cytotoxic activity.

2.1 Investigation of the dimerisation of Oxaliplatin and Carboplatin in solution

Diffusion-ordered ^{1}H NMR spectroscopy (^{1}H DOSY NMR)[22] is a tool of choice for the structural analysis of macromolecular systems, it enables in some cases the collection of important structural information on small molecular systems. [18,23] In the case of solutions of **1**, **2** and **3** the formation of oligomers could not be established. Large variations of the concentration of analyte within the limits of their solubility, did not induce major changes of the measured hydrodynamic diffusion coefficient, which indicated that DOSY was ineffective partly due to the inaccuracy that resides in the very definition of the *hydrodynamic volum*e included in the *Stoke-Einstein* equation; this volume is not related directly to analyte's volume that one can approximate, for instance, by the solvent-exclusion van der Waals volume of a molecule.[23] Another attempt to demonstrate the formation of a $[\mathbf{1}]_2$ dimer in water by measuring the variations of absorbance *A* of the UV-vis absorption spectrum of **1** as a function of analyte's concentration *c* was inconclusive. Namely, it failed to provide the expected non-linear variation of the $A=f(c)$ curve generally symptomatic of the formation of a dimer, thus confirming early observations by Dabrowiak.[7] Noteworthy, the concentration was constrained within the 1-10 mM domain by the poor solubility of **1** in water.

Further investigations of the self-association were consequently restricted to the almost planar complexes **1** and **2** in water using the methods of isothermal titration calorimetry (abbr. ITC), which allows the accurate determination of thermodynamic parameters such as enthalpy of formation/dissociation of oligomers. These parameters are generally produced by the numerical treatment of thermographic traces, applying appropriate thermodynamic models.

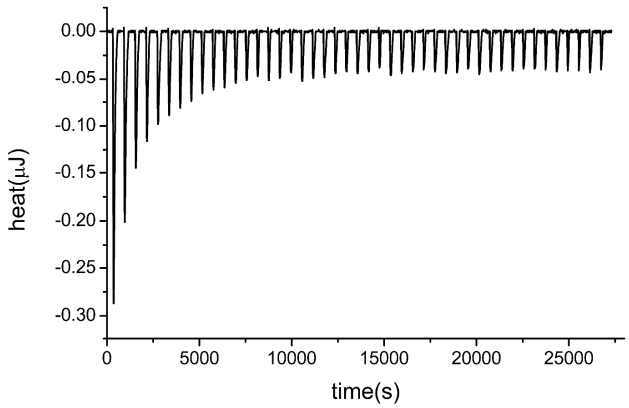

Figure 2. ITC thermograph of the dilution by sequential additions of a concentrated aqueous solution of **2** (c = 20 mM, v= 2.06 μL) in pure water at 25 °C; heat release is expressed in μJ vs. time in s.

For instance, the dissociation of hypothetical dimers $[\mathbf{1}]_2$ and $[\mathbf{2}]_2$ was investigated by the dilution of 20 (**2**) to 10 mM (**1**) aqueous solutions of analyte into a relatively large volume of pure water by applying the method of Young et al.[24, 25]

$$2\,\mathbf{1} \rightleftharpoons [\mathbf{1}]_2 \qquad K_1=\frac{c_{[1]_2}}{c_1^2}$$

$$2\,\mathbf{2} \rightleftharpoons [\mathbf{2}]_2 \qquad K_2=\frac{c_{[2]_2}}{c_2^2}$$

$$\mathbf{1} + \mathbf{2} \rightleftharpoons [\mathbf{1.2}] \qquad K_{12}=\frac{c_{[1.2]}}{c_1 \times c_2}$$

$$c_1^0 = \underbrace{c_1 + c_{[1]_2}}_{c_1^*} + c_{[1.2]}$$

$$c_2^0 = \underbrace{c_2 + c_{[2]_2}}_{c_2^*} + c_{[1.2]} \qquad K_{12}^*=\frac{c_{[1.2]}}{c_1^* \times c_2^*}$$

Figure 3. Formulations of association constants.

For compound **1**, ITC experiments gave no noticeable endothermic heat flow above the dilution background trace, which, in other terms, suggests that either the proportion of oligomer(s) in solution or the enthalpy of dissociation was too low to produce sensible heat flow.

For compound **2**, a typical endothermic trace was recorded (Figure 2) which matched, assuming dimer dissociation within Young's model, [24, 25] a value of +0.46 ± 0.08 kcal/mol for the enthalpy of dissociation ΔH_{dis} at 298.15 K (the enthalpy of dimer formation ΔH_{f} has the opposite sign, i.e -0.46 kcal/mol) and a monomer-dimer association constant K_2 (Figure 3) of ca. 3×10^{-4}. The latter value corresponds to an approximate Gibbs energy ΔG_{f2} of ca. +4.6 kcal/mol and a value of entropy change ΔS_{f2} of ca. -17 cal/K.mol. Compounds **1** and **2**, which differ only by the nature of the metal and by few structural features, were probed for their possible mutual interaction. Titration was performed by mixing, in serial microinjections, equimolar solutions (10 mM) of **1** and **2**. The resulting thermographic trace provided a clear exothermic behaviour (Figure 4). Curve fitting assuming an idealized equilibration between **1** and **2** on the one hand and [**1•2**] on the other hand provided an enthalpy of association of -0.56 kcal/mol at 298.15 K and a value of 5.1×10^{-4} for the apparent constant of association K_{12}^* (Figure 3). The latter is defined as shown in Figure 4, it is associated with a Gibbs energy ΔG_{f12} value of +4.5 kcal/mol at 298.15 K and an entropy change of -17 cal/K.mol if one assumes the proportions of $[\mathbf{1}]_2$ and $[\mathbf{2}]_2$ to be negligible.

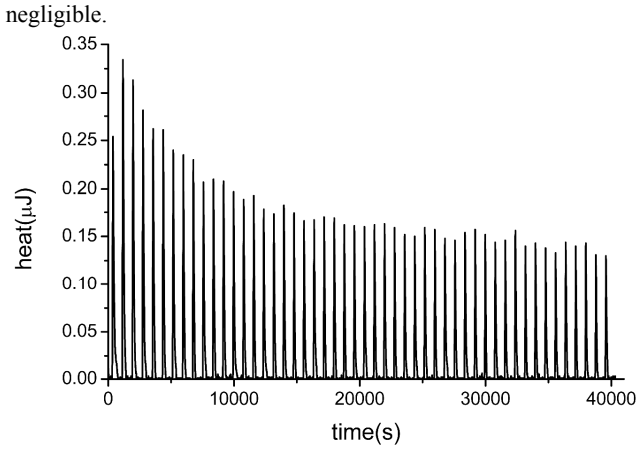

Figure 4. Thermograph of the titration of a solution of **1** (c_1^0= 10 mM) by sequential additions of a solution of **2** (c_2^0= 10 mM, v= 4.00 μL) at 25 °C; heat release is expressed in μJ vs. time in s.

2.2 Oligomers in the gas phase

In quite good agreement with earlier reports by other authors,[7,12] it was found that compounds **1-3** do produce oligomers in the gas phase. Under the mild conditions of electrospray ionisation (ESI) in the presence of traces of formic acid and of sodium salts, all three compounds produced complex features in the positive ion mode.

Whether water or DMSO was used as solvent, no difference in the ESI+ mass spectrum could be noticed. Figures 5 and 6 show the presence of rather intense signals assigned to oligomeric forms associated to either a proton or a sodium ion. The variety of "nuclearities", that is the number of monomeric unit per oligomer, that are achieved under such conditions can be deduced from analysis of the isotopic distribution of the main peaks, which reveals that dimers, trimers, tetramers and hexamers readily form in the gas phase with **1-3** (cf. ESI page S4 for spectra of **3**). Peaks assigned to double cationic tetramers and hexamers of **1** were found hidden behind the isotopic pattern of the respective monocationic dimers and trimers that have identical averaged *m/z* ratio.

The latter results inform of the obvious propensity of **1-2** to self-assemble in the gas phase into cationic species of sufficient life-time to allow detection.

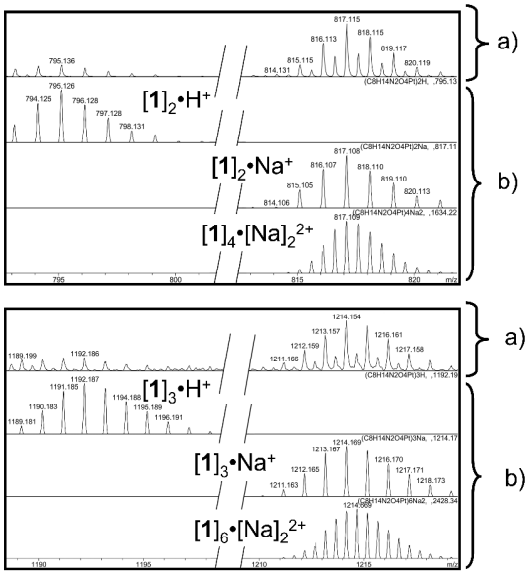

Figure 5. Selected regions of the ESI+ mass spectrum of a water solution of **1** containing traces of formic acid and trace contamination by Na^+ salts: a) experimental spectrum, b) simulated isotopic patterns.

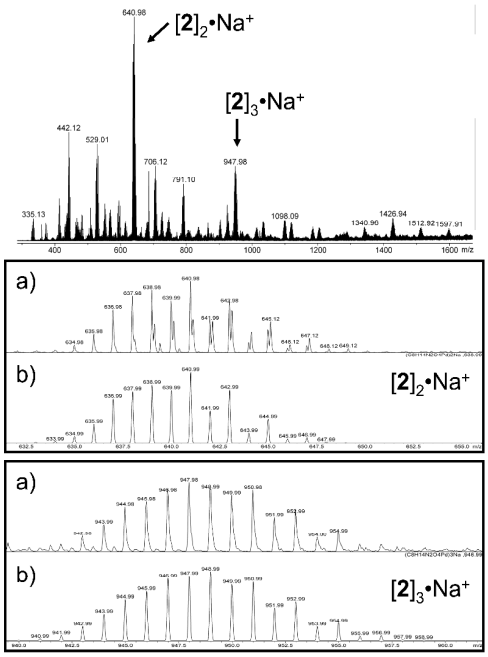

Figure 6. Selected regions of the ESI+ mass spectrum of a water solution of **2** containing traces of Na^+ salts: a) experimental spectrum, b) simulated isotopic patterns.

2.3 In *vacuo/solutio* DFT study of oligomerization

The aggregation of **1-3** in either the gas phase or solution was modeled by taking advantage of the first-principles-based DFT-D3 approach[15], which was designed to treat, in a physically correct manner, the attractive contribution of the London force, also known as *dispersion,* in addition to all other inter and intra-molecular interactions properly treated by conventional DFT.

All dispersion corrections reported refer to the zero-damping version of D3 (a.k.a. D3(0)). The differences to the later published so-called Becke-Johnson (BJ) damping approach (a.k.a. D3(BJ))[26, 27] are small and do not affect any of our conclusions (vide infra).

Models of oligomers of **1-3** were inspired partly by the structures obtained by X-ray diffraction analysis, which are deposited with the CSDB.[14] However, whereas most of the experimental crystal structures tend to point a preference for side-to-side γ-type association (Figure 7) leading to an organisation in parallel strands,[28] theoretical calculations *in vacuo* as well as with a model of solvation (vide infra) indicated that the stacked arrangement β observed in one experimental structure of a similar complex by Galanski et al.[14] leads to optimal stabilisation. In the following sub-sections three arrangements are considered as they came out of geometry optimizations at the (ZORA)[29] BLYP[30, 31]-D3(0)/all electron[32]-TZP level as local minima. These are namely the head-to-tail stack α, the head-to-tail shifted-stack β and the side-to-side γ arrangement (Figure 8). The α and β arrangements differ by the angle of the normal to the chelate mean plane embodied by the M-M axis, which in the former arrangement (α) is close or equal to 90 deg and different from this value in the latter arrangement (β).

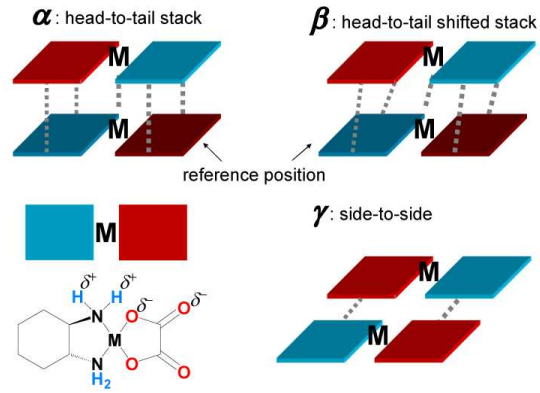

Figure 7. Symbolic representations of the arrangements of the aggregates in local energy minima for head-to-tail dimers of **1-3**. The blue coloured plate represents the amine ligand and the red colored to the carboxylate ligand. Dotted lines symbolize non-covalent interactions and H-bonds supposedly intervening in the cohesion of the arrangement.

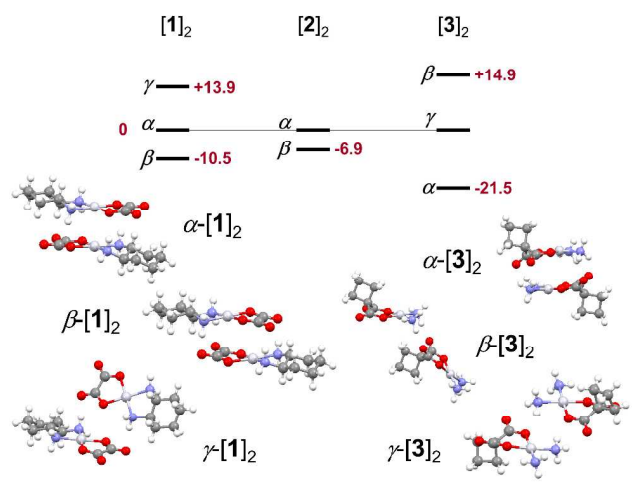

Figure 8. Relative energies of the α, β and γ arrangements of the gas-phase dimers of **1-3** (in kcal/mol); cf. ESI for details.

Inspection of the energies of those three types of arrangements indicate that the most favored one is the β for $[\mathbf{1}]_2$ and $[\mathbf{2}]_2$ by ca. 10 and 7 kcal/mol respectively. Formation energies ΔE_f for those

two dimers in the gas phase are by ca. 10 and 7 kcal/mol more favorable to the β arrangement than to the α (Figure 9). The situation is slightly different in the case of **3**, partly because of the steric strain induced by the cyclobutyl fragment. In this case, the α arrangement, i.e α-[**3**]$_2$ appears to be favored. The β-[**3**]$_2$ has nothing in common with those of the dimers of **1** and **2** because at least two main N-H…O interactions are missing, which makes it the least favored arrangement here. This trend is corroborated by Energy Decomposition Analyses (EDA),[33,34] which indicate (Table 2) that the largest intrinsic interaction energies between prepared monomers are found for β-[**1**]$_2$, β-[**2**]$_2$ and α-[**3**]$_2$.

Table 2. Components (in kcal/mol) of the Energy decomposition analysis (EDA) for geometries of gas-phase dimers of **1-3** computed at the ZORA-BLYP-D3(0)/all electron TZP.

Complex	ΔE_{def} (kcal/mol)[a]	ΔE_{int} (kcal/mol)	ΔE_f (kcal/mol)
α–[**1**]$_2$	+5.4	-60.4	-55.0
β–[**1**]$_2$	+7.9	-73.4	-65.5
γ–[**1**]$_2$	+3.2	-44.2	-41.1
α–[**2**]$_2$	+4.6	-57.6	-52.9
β–[**2**]$_2$	+8.0	-67.9	-59.9
α–[**3**]$_2$	+15.4	-73.9	-58.5
β–[**3**]$_2$	+2.5	-24.6	-22.0
γ–[**3**]$_2$	+4.2	-41.3	-37.0

[a] within the EDA scheme, ΔE_{def} (>0) corresponds to the deformation energy necessary to prepare each fragment before interaction, ΔE_{int} (generally <0) is the interaction energy, ΔE_f is the formation energy: $\Delta E_f = \Delta E_{int} + \Delta E_{def}$.

Breaking down ΔE_{int} into its main Pauli, orbital, electrostatic and dispersion components informs of the peculiar importance to the latter term, which amounts to 27 %, 39 % and 49 % of the total interaction energy in γ-[**1**]$_2$ (ΔE_{int} = -44.0 kcal/mol), β-[**1**]$_2$ (ΔE_{int} = -73.4 kcal/mol) and α-[**1**]$_2$ (ΔE_{int} = -60.1 kcal/mol) respectively. It is interesting to note that the L…L contribution to the total dispersion is ca 55%, and M…M only ca 5% in the case of α-□[**1**]$_2$ and 55% (L…L); 8% (M…M) in the case of □β-[**1**]$_2$. Similar results were obtained for the other complexes (ESI, section 6.2, page S25). Particularly in the case of β-[**1**]$_2$ and β-[**2**]$_2$, the larger ΔE_{int} value results from more favorable electrostatic and orbital terms, which can be assigned to the H-bonding that constitutes a major effect responsible for the cohesion of those dimers in the gas phase.

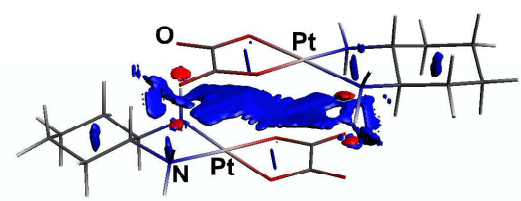

Figure 9. ADFview2013 plots of non-covalent interaction (NCI) regions indicated by *reduced density gradient* isosurfaces (cut-off value s= 0.02 a.u., ρ= 0.05 a.u.) coloured according to the sign of the signed density $\lambda_2\rho$ (red and blue colours are associated to negatively and positively signed terms) for the gas-phase relaxed singlet ground state model of Pt-containing complexes β-[**1**]$_2$. All calculations were performed with gas phase singlet ground state optimized geometries at the ZORA-BLYP-D3(0)/all electron TZP level. Non-covalent N-H…O bonds are indicated by attractive non-covalent red-coloured isosurfaces. Blue isorsurfaces are assigned to van der Waals interactions or to Pauli repulsion .

The orbital interaction energy term was decomposed in the cases of β–[**1**]$_2$ and β–[**2**]$_2$ using the NOCV-ETS method developed by Mitoraj, Michalak and Ziegler.[35] This analytical method, which allows a symmetry-ordered decomposition of interfragment orbital interactions, provided a clear picture of the contribution of H-bonding in the cohesion of the gas-phase dimer and confirmed the absence of any significant metal-metal orbital interaction (Wiberg bond indices[36] $w_{M\text{-}M}$ < 0.05) (cf. ESI page S30). In both cases, only three orbital interaction terms were found to relate to NH…O hydrogen bonds with values of *ca.* 5 kcal/mol, a rather low value consistent with the lack of obvious synaptic basins in between the fragments noted in the analysis of the Electron Localisation Function (abbr. ELF).[37] Worthy to note in the case of both β-[**1**]$_2$ and [**2**]$_2$, the anchoring effect of H-bonding can be visualized by Yang's Non-Covalent Interaction (abbr. NCI) regions,[38,39] an intuitive analysis of the electron density topology based on a strict discrimination of the reduced density gradient between covalently bonded and non-covalently interacting atoms. The red coloured isosurfaces (Figure 9, β-[**1**]$_2$ shown here) materialize the attractive intermolecular amine-carbonyl H bonds. Also worthy, the HOMO-LUMO energy gaps of dimers β–[**1**]$_2$ ($|\Delta E_{monomer\text{-}dimer}|$ = 0.35 eV), β–[**2**]$_2$ ($|\Delta E_{monomer\text{-}dimer}|$ = 0.42 eV) and α-[**3**]$_2$ ($|\Delta E_{monomer\text{-}dimer}|$ = 0.16 eV) are only slightly different from those of the parent monomers, which explains mostly why no major changes are observed in the solution UV-vis spectra upon dilution of concentrated solution of **1** if its supposed dimer forms, which disqualifies UV-vis titration as a method of characterization (cf. ESI page S15).

Comparison of the BLYP-D3(BJ) energies with those of TPSS-D3(BJ), a notoriously suitable functional for systems with transition metals,[40-42] and of wavefunction-based CCSD(T)/CBS, a "golden standard"[43] were performed on a small model of a Pt chelate dimer devoid of H-bonds (cf. ESI, Figure S50) of formula $[(NH_3)_2Pt(HC(O)C(O)H]_2$. BLYP–D3(BJ) and TPSS-D3(BJ) methods showed good agreement with CCSD(T)/CBS for this small system; BLYP-D3(BJ) overestimated interaction energy by 0.4 kcal/mol, and TPSS-D3(BJ) by 0.6 kcal/mol compared to the limit estimated by CCSD(T)/CBS (-1 kcal/mol) (cf. ESI Table S4)

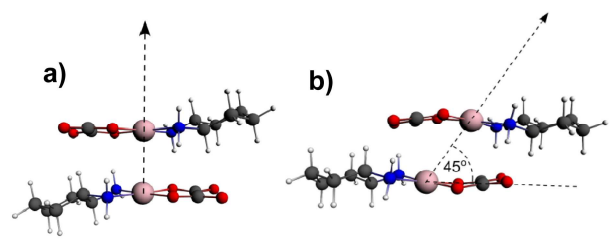

Figure 10. Axes along which the position of each fragment was shifted to the potential energy curves on a rigid model of [**1**]$_2$: a) excursion along the normal to the chelate's mean plane in the α configuration ; b) excursion along the axis defined by the Pt-Pt segment that forms an angle of ca. 45° with chelate's mean plane.

This result provided stable ground for using further the computationally-light BLYP-D3 method, a conclusion further consolidated by comparing the potential energy curves (PECs) computed with BLYP-D3(0), BLYP-D3(BJ), TPSS, TPSS-D3(BJ) and the non-local density-dependent version of TPSS, i.e TPSS-NL(VV10)[44] in which the dispersion energy is computed from the electron density using the modified approach of Vydrov

and van Voorhis.[45] The PECs of α and β arrangements of [**1**]$_2$ and [**2**]$_2$ were computed considering rigid fragments, which were translated along the axes defined by the M-M segment in the energy minimum (Figure 10).

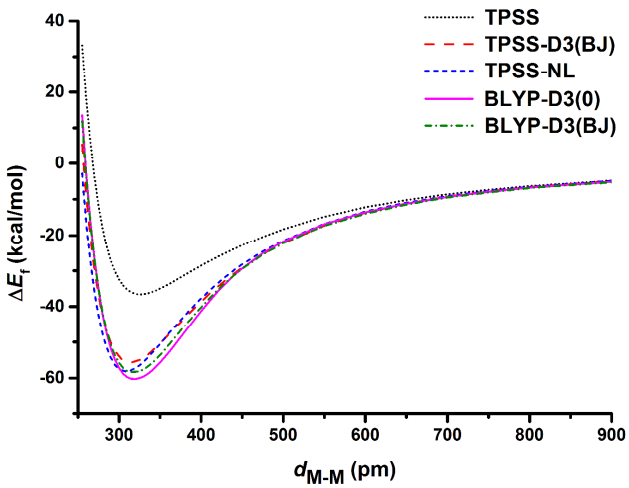

Figure 11. Potential energy curves (PEC) for α-[**1**]$_2$ (M= Pt) drawn for a selection of functionals. Computations with TPSS (native, -D3(BJ) and -NL) were carried out with a def2-TZVP basis set.

As shown in Figure 11 the BLYP-D3(0) and –D3(BJ) functionals produce PECs with minima and asymptotic behaviours very similar to that produced by TPSS-NL, the latter yielding a slightly shorter $d_{M\text{-}M}$ value at its energy minimum. As can be seen from Figure 11, adding the dispersion energy to the standard TPSS result has a large and non-negligible effect on the interaction. Moreover, the equilibrium region is lower by around 12 kcal/mol which is about 25 % of the entire interaction even in this polar system involving also hydrogen bonding. This, once again, demonstrates the importance of dispersion also for systems which are normally not associated with dispersion (van der Waals) type interactions.

Worthy to note, the PECs produced by TPSS-D3 and the density-dependent TPSS-NL dispersion model (Figure 11) are directly comparable regarding the dispersion effect. As can be seen, both methods agree very well over the entire distance range which strongly supports our overall approach. Note that this is non-trivial as the dispersion coefficients in D3 for metal atoms are computed from reference molecules (element hydrides). This approach works very well for non-metallic elements but due to larger changes in oxidation state, it may be less accurate in metallo-organic systems. Nevertheless, in this case the dispersion interactions, and in particular those involving the Pt atoms, seem to be described well at both levels of theory.

BLYP-D3 results in Figure 11 merely demonstrate that the functional dependence of the interaction is relatively weak and that the choice of the damping function in D3, i.e (BJ) or (0), is of no importance.

Modeling the polarity effect of the surrounding solvent was performed using the COSMO solvation model[46-48] in a first instance. The PECs of the α and β arrangements (not shown here) where compared in the solvent continuum of DMSO (COSMO) as a way to discard the arrangements associated with an incorrect asymptotic behaviour. This study, carried out with α- and β-[**1**]$_2$ revealed that the former arrangement leads to unviable dimers in DMSO, whereas the latter produced better asymptotic behaviour, suggesting persistence of the dimer in solution. The effect of solvation on the Gibbs energy of formation of those molecular aggregates is important. Table 3 lists the main thermodynamic parameters for the formation of [**1**]$_2$, [**2**]$_2$ and [**1**,**2**]. Solvation leads to an absolute decrease of the formation Gibbs energy of about 30 kcal/mol. In all cases the α arrangement leads to positive values of ΔG_f^{298} whereas the β arrangement is generally associated with negative values. The excursion of theoretical data from experimental ones is rather limited and overall acceptable given that basis set superposition error (BSSE) was not accounted for in the values listed in Table 3. BSSE calculated by the counterpoise method (CP)[49], which was computed for the (COSMO) relaxed geometries represents about 2.5 % of the computed interaction energy between the two fragments, which brings the corrected ΔG_f^{298} for β-[**2**]$_2$ into a slightly positive value and a decrease in absolute value ΔG_f^{298} for β-[**1**]$_2$. Lack of consideration for the specific interactions of water with the solute by the solvation model used here (COSMO) can also be held responsible for the observed discrepancies between theory and experiment; theory overestimating the propensity of the system to self-assemble.

Table 3. Calculated thermodynamic parameters for various combinations of monomers, in the gas phase as well as with a COSMO solvation treatment (BSSE not accounted).

entry		ΔH_f^{298} kcal/mol	ΔS_f^{298} kcal/mol.K	ΔG_f^{298} kcal/mol
1	exptl [**1**]$_2$ (water)[a]	*na*[b]	*na*	*na*
2	α–[**1**]$_2$	-53.4	-0.054	-37.4
3	β–[**1**]$_2$	-63.3	-0.057	-46.5
4	β–[**1**]$_2$-(DMSO)	-20.0	-0.042	-7.4
5	α–[**1**]$_2$-(water)	-15.6	-0.060	2.2
6	β–[**1**]$_2$-(water)	-18.9	-0.037	-7.7
7	exptl [**2**]$_2$ (water)[a]	-0.5	-0.017	+4.6
8	α–[**2**]$_2$	-50.6	-0.050	-35.6
9	β–[**2**]$_2$	-56.8	-0.042	-44.0
10	β–[**2**]$_2$-(DMSO)	-17.0	-0.053	-1.3
11	β–[**2**]$_2$-(water)	-16.4	-0.051	-1.1
12	exptl [**1•2**] (water)[a]	-0.6	-0.017	+4.5
13	β–[**1•2**]	-60.2	-0.051	-45.1
14	β–[**1•2**] (water)	-18.5	-0.043	-5.6

[a] from ITC experiments. [b] not available

2.4 DFT-D vs. calorimetry for *in solutio* systems, a tentative comparison

A way to probe the pertinence of the theoretical models is to compare the computed thermodynamic parameters with those obtained for a standard non-covalent association process obtained by ITC in solution. This approach is however limited by the

treatment of solvation in conventional DFT methods. We will present in the following a first approach making use of two conventional solvation models, namely COSMO and COSMO-RS.

Inclusion of coordination complexes into the lipophilic cavity of cucurbit[*n*]urils (abbreviated **CB**[*n*]) was already well documented; the thermochemistry of such non-covalent association process particularly suits the sensitivity of ITC.[50,51] It was shown recently that a pertinent reproduction of experimental association thermodynamic parameters of rather large molecular systems not only required the use of dispersion-corrected functionals but also the inclusion of the three-body dispersion energy term.[51]

2.4.1 Thermochemical data

With complex **1,** for which the inclusion host-guess complex, i.e **1**@**CB**[7], was also crystallographically characterized, Kim and co-workers[50] provided some information on the thermodynamics of the inclusion process by reporting an enthalpy ΔH of -6.3 ± 0.1 kcal/mol at p*H*= 7.2 in the presence of TRIS buffer at 25 °C with an association constant K of 2.3×10^5. To this value was also associated an entropy variation ΔS of +3.3 cal/mol.K. Even though the authors did not indicate the exact concentration of TRIS in their experiments, it is very likely that it acted as a guest competing with **1** for inclusion into **CB**[7]. This introduced, in our opinion, a serious risk of underestimation of the actual affinity of **1** for the considered cavitand.

For the purpose of comparison and in order to show the influence of TRIS on the inclusion process, we performed ITC titrations of a solution of **CB**[7] in a commercially available 200 mM TRIS buffer with a solution of **2** prepared in the same TRIS buffer, as well as titrations with pure water solutions of **1** and **2** and **CB**[7].

Table 4. Thermodynamic data extracted from isotherm titration calorimetry investigations of the reactions of **1** and **2** with **CB**[7].

cmpd	**1**	**1**	**2**	**2**
solvent	water	water	water	water+TRIS
T (K)	298.15	313.15	298.15	298.15
ΔH_{raw} [a] (kcal/mol)	-7.8(2)	-10	-6.2(3)	-1.62(2)
ΔH_{mod} (kcal/mol)	-8.7(2) [b]	-10.9 [b]	-6.6(5) [b]	-6.6(5) [c]
ΔH_{TRIS} (kcal/mol)				-5.0(2)
K_1	$2.4(6)\times10^5$	9×10^5	$0.7(3)\times10^5$	$0.7(3)\times10^5$ [d]
K_2				34(6)
ΔS_{mod} (cal/mol.K)	-4.73(5)	-7.5	0(2)	
ΔS_{TRIS} (cal/mol.K)				-10(1)
ΔG_{mod} (kcal/mol)	-7.3(1)	-8.5	-2.1(1)	-

[a] enthalpy of the process computed from the net heat released by the process corrected relative to a blank experiment consisting of an injection of complex into a solvent devoid of **CB**[7]. [b] the numerical model applied here, i.e the MSCBS, was that of a host-guest interaction between independent molecules. [c] the numerical model applied here was that of competitive replacement of ligand, whereby the competing process of inclusion of TRIS is characterised by ΔH_{TRIS} constant K_2 and ΔS_{TRIS}. [d] values of ΔH_{mod} and K_1 determined in pure water were entered as constants for the determination ΔH_{TRIS} and K_2.

Treatment of the ITC data for the inclusion of **1** (20 mM) into **CB**[7] (0.74 mM) in pure water using the model of *multiple set of independent binding sites*[52] (abbr. MSCBS) provided an enthalpy of inclusion ΔH_{mod} of -8.7(1) kcal/mol at 298.15K and an association constant K_1 of $2.4\cdot10^5$. Similar treatment of the data related to the inclusion of **2** (17 mM) into **CB**[7] (1 mM) in pure water afforded an enthalpy of inclusion ΔH_{mod} of -6.6(5) kcal/mol at 298.15K and an association constant K_1 of $7\cdot10^4$.

Given the high values of the computed association constants K_1, the self-consistency of the thermochemical model was checked by calculating the raw enthalpy of association ΔH_{raw} by integrating the total molar heat release from the ITC thermograph: the resulting values of -7.8 and -6.2(3) kcal/mol for the formation of **1**@**CB**[7] and **2**@**CB**[7] respectively validated the chosen thermochemical model.

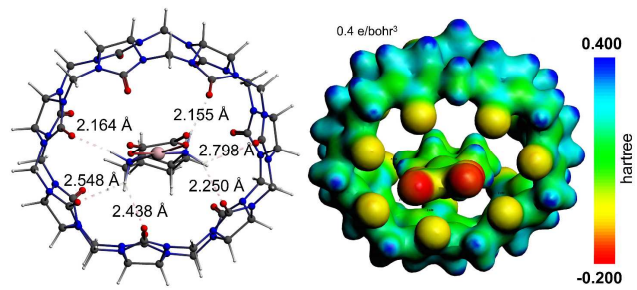

Figure 12. The relaxed COSMO (water) geometry of inclusion complex **2**@**CB**[7]: left, outline of the shortest NH…$O_{CB[7]}$ contacts within the cucurbit[7]uril's cavity ; right, coulombic potential map drawn over an isosurface of the electron density.

Worthy to note, experiments with TRIS-buffered solutions (200 mM) revealed the relevant interference of this amine with the inclusion process of **2** (20 mM) into **CB**[7] (1 mM). As a blind test, the above-mentioned MSCBS model was applied and a value of -1.97(6) kcal/mol for ΔH_{mod} was obtained along with a K_1 constant of $1.6(2)\cdot10^4$. It became obvious that TRIS was playing the role of a competing guest of **CB**[7] and that the effect of its concentration in the medium had to be accounted for. The treatment of ITC data using the "*Competitive Replacement*"[53, 54] (abbr. CR) model, assuming TRIS as a competitor of **2** (for which the enthalpy and constant of association were priorily determined) in the binding with **CB**[7], yielded an enthalpy of association of TRIS with **CB**[7], i.e ΔH_{TRIS}, of -5.0(2) kcal/mol and a value of 34(6) for the constant of association of TRIS with **CB**[7]**,** i.e K_2 (Table 4).

2.4.2 DFT-D computations

Our computation of the thermodynamics of inclusion complexes[51] was carried out with geometries optimized with a COSMO treatment of solvation from the cartesian coordinates of Kim's first structure[50] of **1**@**CB**[7] which was used here to build also the model of **2**@**CB**[7] (Figure 12). Those geometries were subsequently applied a COSMO-RS[55] treatment to determine the Gibbs free enthalpies of solvation that would yield the $\Delta\delta G_{solv}$ parameter used to approximate the values of the Gibbs free enthalpy of formation of the inclusion complex in idealized water from monomers **1-2** and **CB**[7] by applying the following :

$$\Delta G_f(\text{water}) = \Delta E_g + \Delta G_{RRHO} + \Delta\delta G_{solv} + \Delta E^{(3)}{}_{disp} + \Delta E_{BSSE}$$

where ΔE_g is the host-guest association energy for COSMO-relaxed geometries taken in the gas phase, ΔG_{RRHO} is the rigid rotor harmonic oscillator energy correction from E to G taken for gas phase calculations, $\Delta E^{(3)}{}_{disp}$ is the three-body dispersion energy term and ΔE_{BSSE} is the energy correction for the so-called basis set superposition error.[49] Table 5 gathers the values computed in the gas-phase and in idealized water (COSMO-RS).

Table 5. Estimate of the thermodynamic parameters for the inclusion of **1** and **2** into **CB**[7] in the gas-phase (ZORA-BLYP-D3(0)/all electron TZP) and in water (COSMO geometries, treated with COSMO-RS) (energies in kcal/mol).

Gas-phase	ΔE_f	ΔH_f	ΔS_f	ΔG_f^{298}
1@CB7	–49.6	–48.9	–0.065	–29.4
2@CB7	–48.9	–47.6	–0.058	–30.2

COSMO-RS water	ΔE_g	ΔG_{RRHO}	$\Delta\delta G_{solv}$	$\Delta E^{(3)}_{disp}$	BSSE	ΔG_f^{298}
1@CB7	-47.4	20.2	8.5	4.6	1.6	-12.3
2@CB7	-47.4	18.7	8.9	4.7	1.5	-13.6

In the herewith considered model of inclusion complex the role of explicit water was neglected for computational practical reasons. However this was done knowing that, particularly for aqueous solutions of **CB**[7], the inclusion of any guest within the cucurbituril is challenged by the existence, within the cavity itself, of metastable so-called "high energy water" aggregates[56]. The latter supposedly form, according to the assumptions of Nguyen, Young and Gilson[57], a high density low-entropy water torus that only the interaction with highly hydrophobic guests can displace, provided that an energy toll of ca. 9-15 kcal is paid in the water-displacement free energy. In the case of **1** and **2**, which are both moderately lipophilic and rather keen to establish specific interactions with bulk water, the values of affinities for **CB**[7] computed by combining DFT-D and COSMO-RS solvation model remain in reasonable agreement with experimental data, particularly if one considers that a negligible energy toll must be paid for the dissociation of portions of dimers $[\mathbf{1}]_2$ and $[\mathbf{2}]_2$. Considering that the theoretical ΔG value is a sum of individually large terms of opposite sign, which have been computed without any specific empiricism, the computed correct sign and right order of magnitude for ΔG seems to be a respectable result. Because the δH_{solv} values are indirect quantities for which the COSMO-RS model was not developed, enthalpy of solvation was not sought.

Our approach provides an insight that differs fundamentally from another recently published report[58] in which the inclusion of cis-platin type complexes into **CB**[7] was carried out using the hybrid B3LYP functional[59] in spite of the notorious tendency of this dispersion correction-devoid hybrid functional to raise major BSSE issues.[60,61,62]

3. Conclusions

From a combination of physical methods and theoretical treatments this study provides evidence for the formation of dimers, if not oligomers, of compounds **1-3** in the gas phase. This propensity to self-aggregate is primarily due in the gas phase to the ability of the compounds in question to establish H-bonds, which is challenged by the specific interactions of bulk water in solution. Hence, the non-local attractive dispersion force most likely assists H-bonding in the dimerization process in solution by counter balancing the entropic penalty induced by hydration; the significant lipophilicity of **1** and **2** was well gauged by the measured affinity of those chelates for cucurbit[7]uril. This contribution of dispersion is particularly obvious in the inter-fragment interaction energy of dimers $[\mathbf{1}]_2$ and $[\mathbf{2}]_2$. The fact that the shifted stacked β arrangement seems to be particularly favored in solution for **1** and **2** questions the role of electron correlation-based metal-metal attractive interactions, which was not addressed here. This study outlines the performance of DFT-D in producing rather realistic thermodynamic parameters,[60,63] in spite of known limitations placed by implicit solvation models. The main goal of this study was to provide a full investigation of the suspected aggregation of Oxaliplatin in concentrated infusion, which has long been correlated with its unexpected stability towards hydrolysis. Our investigations suggest that monomeric Oxaliplatin tends to be rather preponderant at least in solution in pure water. In the scope of the development of anti-cancer drugs that can withstand storage over long periods of time in aqueous media, the correlation of resistance towards hydrolysis with self-aggregation remains an open question.

4. Experimental section

General

Pure water was obtained by reverse osmosis using a Millipore Ri0s-v5 water purification system. Deuterated solvents were dried over sodium or CaH_2 and purified by trap-to-trap techniques, degassed by freeze-pump-thaw cycles and stored under argon. ^{1}H, ^{13}C NMR spectra were obtained on Bruker DPX 300, 400 or Avance 500 spectrometers. Chemical shifts were referenced in parts per million (ppm) against solvent peaks or external references. Carboplatin (**3**) and Oxaliplatin (**1**) were purchased from TCI Europe, and were used as received without further purification. Compound **2**[28,64] and cucurbit[7]uril (**CB**[7])[65] were prepared and purified according to literature procedures.

Diffusion ordered spectroscopy (DOSY)

Measures of self-diffusion coefficients were performed on a BRUKER 600 MHz spectrometer - Avance III, equipped with a high strength ***z*** gradient probe DOTY Scientific. Diffusion NMR data were acquired using a Stimulated Echo pulse sequence with bipolar z gradients. DOSY spectra were generated by the DOSY module of the software NMRNotebook, using Inverse Laplace Transform (ILT) driven by maximum entropy, to build the diffusion dimension. Hydrodynamic radii were calculated using Stokes-Einstein equation from diffusion coefficients determined by NMR and viscosity values of solvents used.[23]

Isothermal titration calorimetry

All measures were carried out with a Waters-SAS nanoITC device equipped with two stainless steel hastealloy cells of 1 mL volume each. All aqueous solutions were prepared by sonication of suspensions of the complexes in pure water and were subsequently thoroughly degassed under reduced pressure.

Mass spectrometry

MALDI-TOF mass spectra were acquired on a time-of-flight mass spectrometer equipped with a nitrogen laser.

ESI-MS experiments were performed on a Bruker Daltonik GmgH (Bremen, Germany) microTOF spectrometer equipped with an orthogonal electrospray (ESI) interface. Calibration was performed using Tuning mix (Agilent Technologies). Sample solutions were introduced into the spectrometer source with a syringe pump (Harvard type 55 1111: Harvard Apparatus Inc., South Natick, MA, USA) with a flow rate of 5 $\mu L.min^{-1}$. An external multi-point calibration was carried out before each measurement using the singly charged peaks of a standard peptide mixture (0.4 µM, in water acidified with 1% HCOOH). Scan accumulation and data processing were performed with FlexAnalysis 3.0 software. α-Cyano-4-hydroxy-cinnamic acid (CHCA) was obtained from Sigma (St Louis, MO, USA), 1,8,9-anthracenetriol (dithranol) from Alfa Aesar (Karlsruhe, Germany). Matrix solutions were freshly prepared: CHCA was dissolved to saturation in a $H_2O/CH_3CN/HCOOH$ solution and dithranol to saturation in THF. Typically, a 1/1 mixture of the sample solution in CH_2Cl_2 was mixed with the matrix solution and 0.5 µL of the resulting mixture was deposited on the stainless steel plate.

Computational details

Computations were performed by DFT methods using the "zero damped" dispersion-corrected Becke[30]-Lee-Yang-Parr[31] (BLYP- D3[15], D3-BJ[26,27]) functionals implemented in the ADF®: Amsterdam Density Functional package (ADF2012.01).[66,67] Scalar relativistic effects were treated within the Zeroth Order Regular Approximation (ZORA)[29], with all-electron (AE)[32] ZORA/TZP, ZORA/TZ2P and ZORA/QZ4P basis sets were used. Larger basis sets (TZ2P, QZ4P) were used for checking the final geometries against the optimal TZP basis set. Because the changes in the final geometries were minimal, larger basis sets were not used further. All calculations were done in gas phase, unless stated otherwise. Geometry optimizations by energy gradient minimization were carried out in all cases with the C_1 and C_2 point group symmetries, where the differences in the energies obtained for the same system were negligible. Integration grid accuracy spanned 4.5-6, the energy gradient convergence criterion was set to 10^{-3} au, and tight SCF convergence criteria (10^{-7} au) were used. Inter-fragment Kohn-Sham orbital interaction analyses were performed with optimized geometries within the ADF package. Wiberg bond indices for ADF-optimized geometries (using all-electron TZP basis sets) were computed with the GENNBO 5.0[68] extension of ADF. Solvation by water and DMSO was accounted for using the COSMO procedure with Klamt's values of van der Waals radii for atoms.[46-48] To determine the Gibbs free enthalpies of solvation that would yield the $\Delta\delta G_{solv}$ parameter used to approximate the values of the Gibbs energy of formation of the inclusion complex in idealized water from monomers, COSMO-RS[55] continuum solvation model was used. Thermodynamic parameters were computed from the statistical data, namely internal energy and entropy, generated by vibrational frequency calculations. The latter were computed analytically and by two point numerical differentiation for geometries optimized respectively in the gas phase and in modeled water and DMSO (COSMO). The basis set superposition error (BSSE) was calculated by the counterpoise method (CP).[49] The mixed basis sets are realized by introducing "ghost orbitals", basis set functions which have no electrons or protons. A standard "zero-damping" formula and rational damping to finite values for small interatomic distances according to Becke and Johnson (BJ-damping) have been used for construction of dispersion energy curves. Grimme's DFT-D3 scheme for the computation of the dispersion coefficients was used. ETS-NOCV[35], NCI[38,39] as well as ELF analyses[37] were performed with optimized geometries using ADF2012 and ADF2013 subroutines. Representations of molecular structures and orbitals were drawn using ADFview.

The GAUSSIAN 09, revision B01[69] program was used for calculations of interaction energies ΔE_{int} at the second order Møller–Plesset (MP2)[70] and coupled-cluster single double[71-74](triple)[75] (CCSD(T)) basis set limit level (CCSD(T)/CBS) with frozen core orbitals for metals. The CCSD(T) at basis set limit (CCSD(T)/CBS) energies were estimated by applying the extrapolation scheme proposed by Mackie and di Labio.[76] This scheme uses interaction energies obtained by both accounting and not accounting for the BSSE[77], and calculates average values. The average values obtained by using the MP2 method with aug-cc-pVTZ and aug-cc-pVQZ (with pseudopotential for metal atom) basis sets[78,79] are used to estimate MP2/CBS energies. CCSD(T)/CBS values for the model system were evaluated by assuming that the difference in energies between MP2/CBS and MP2/aug-cc-pVDZ is similar to the difference in CCSD(T)/CBS and CCSD(T)/aug-cc-pVDZ:[80] ΔE(CCSD(T)/CBS)= $\Delta E(\mathrm{CCSD(T)}_{\text{aug-cc-pVDZ}})$ + ΔE(MP2/CBS) - $\Delta E(\mathrm{MP2}_{\text{aug-cc-pVDZ}})$ (cf. ESI, Figure S50 and associated Table)

Acknowledgements

The authors are grateful to the CNRS, the University of Strasbourg, the University of Belgrade, the University of Bonn, the European Doctoral College, the LABEX "Complex Chemical Systems" and the ANR (Projet Blanc 2010 WEAKINTERMET-2DA) for funding and support. Lionel Allouche, Bruno Vincent and Hélène Nierengarten are thanked for their skilfull technical contribution to this work.

Notes and references

[a]Institut de Chimie, Université de Strasbourg, 4 rue Blaise Pascal, 67000 Strasbourg, France. Fax: +33 (0)3 68 85 0001; Tel: +33 (0)3 68 85 15 23; E-mail: djukic@unistra.fr
[b] Faculty of Chemistry, University of Belgrade, 12-16 Studentsky Trg, 11000 Belgrade, Serbia.
[c] Mulliken Center for Theoretical Chemistry, University of Bonn, Beringstr. 4, D-53115 Bonn, Germany. E-mail: grimme@thch.uni-bonn.de
[d] Department of Chemistry, Texas A&M University at Qatar, P. O. Box 23874 Doha, Qatar

† Electronic Supplementary Information (ESI) available: Analytical informations and full listing of cartesian coordinates with energies and vibrational frequencies of all considered models. See DOI: 10.1039/b000000x/

1. in *Cisplatin: Chemistry and Biochemistry of a leading anticancer drug*, ed. B. Lippert, Verlag Helvetica Chimica Acta, Zurich, 1999.
2. S. G. Chaney, S. L. Campbell, E. Bassett and Y. Wu, *Crit. Rev. Oncol. Hematol.*, 2005, **53**, 3–11.
3. M. E. Alberto, V. Butera and N. Russo, *Inorg. Chem.*, 2011, **50**, 6965-6971.
4. I. Ott and R. Gust, *Anticancer Agents Med. Chem.*, 2007, **7**, 95-110.
5. J. Peng, R. Mandal, M. Sawyer and X.-F. Li, *Clin. Chem.*, 2005, **51**, 2274–2281.
6. D. M. Kweekel, H. Gelderblom and H. J. Guchelaar, *Cancer Treatment Rev.*, 2005, **31**, 90-105.
7. A. J. di Pasqua, D. J. Kerwood, Y. Shi, J. Goodisman and J. C. Dabrowiak, *Dalton Trans.*, 2011, **40**, 4821-4825.
8. M. Lederer and E. Leipzig-Pagani, *Int. J. Pharmaceutics*, 1998, **167**, 223–228.
9. M. Pavelka, M. F. A. Lucas and N. Russo, *Chem. Eur. J.*, 2007, **13**, 10108 - 10116.
10. M. F. A. Lucas, M. Pavelka, M. E. Alberto and N. Russo, *J. Phys. Chem. B*, 2009, **113**, 831-838.
11. P. Videhult, J. Yachnin, E. Jerremalm, R. Lewensohn and H. Ehrsson, *Cancer Letters*, 2002, **180**, 191-194.
12. R. B. Burns, R. W. Burton, S. P. Albon and L. Embree, *J. Pharm. Biomed. Anal.*, 1996, **14**, 367-372.
13. M. A. Bruck, R. Bau, M. Noji, K. Inagaki and Y. Kidani, *Inorg. Chim .Acta*, 1984, **92**, 279-284.
14. M. Galanski, A. Yasemi, S. Slaby, M. A. Jakupec, V. B. Arion, M. Rausch, A. A. Nazarov and B. K. Keppler, *Eur. J. Med. Chem.*, 2004, **39**, 707-714.
15. S. Grimme, J. Antony, S. Ehrlich and H. Krieg, *J. Chem. Phys.*, 2010, **132**, 154104.
16. T. Schwabe, S. Grimme and J.-P. Djukic, *J. Am. Chem. Soc.*, 2009, **131**, 14156-14157.
17. C. Werle, M. Hamdaoui, C. Bailly, X.-F. Le Goff, L. Brelot and J.-P. Djukic, *J. Am. Chem. Soc.*, 2013, **135**, 1715-1718.
18. S. Grimme and J.-P. Djukic, *Inorg. Chem.*, 2011, **50**, 2619-2628.
19. S. J. Berners-Price and T. G. Appleton, in *Platinum-Based Drugs in Cancer Therapy*, eds. L. R. Kheland and N. P. Farrell, Humana Press, Totowa, New Jersey, 1999, pp. 3-35.
20. P. D. Prenzler and W. D. McFadyen, *J. Inorg. Biochem.*, 1997, **68**, 279-282.
21. B. Petrovic, Z. D. Bugarcic and R. van Eldik, *Dalton Trans.*, 2008, 807-813.
22. K. F. Morris and C. S. Johnson, *J. Am. Chem. Soc.*, 1992, **114**, 3139-3141.
23. S. E. Harding, *Biophys. Chem.*, 1995, **55**, 69-93.
24. S. D. Burrows, M. L. Doyle, K. P. Murphy, S. G. Franklin, J. R. White, I. Brooks, D. E. McNulty, M. O. Scott, J. R. Knutson, D. Porter, P. R. Young and P. Hensley, *Biochemistry*, 1994, **33**, 12741-12745.
25. G. M. K. Poon, *Anal. Biochem.*, 2010, **400**, 229-236.
26. A. D. Becke and E. R. Johnson, *J. Chem. Phys.*, 2005, **122**, 154104.
27. E. R. Johnson and A. D. Becke, *J. Chem. Phys.*, 2006, **124**, 174104.
28. A. S. Abu-Surrah, T. A. K. Al-Allaf, M. Klinga and M. Ahlgren, *Polyhedron*, 2003, **22**, 1529-1534.
29. E. van Lenthe, A. Ehlers and E.-J. Baerends, *J. Chem. Phys.*, 1999, **110**, 8943-8953.
30. A. D. Becke, *Phys. Rev. A*, 1988, **38**, 3098-3100.
31. C. Lee, W. Yang and R. G. Parr, *Phys. Rev. B Condens. Matter*, 1988, **37**, 785-789.
32. E. van Lenthe and E. J. Baerends, *J. Comput. Chem.*, 2003, **24**, 1142-1156.
33. T. Ziegler and A. Rauk, *Inorg. Chem.*, 1979, **18**, 1558-1565.
34. F. M. Bickelhaupt and E. J. Baerends, *Rev. Comput. Chem.*, 2000, **15**, 1-86.
35. M. P. Mitoraj, A. Michalak and T. Ziegler, *J. Chem. Theory Comput.*, 2009, **5**, 962-975.
36. K. Wiberg, *Tetrahedron*, 1968, **24**, 1083-1096.
37. A. Savin, R. Nesper, S. Wengert and T. F. Fassler, *Angew. Chem., Int. Ed. Engl.*, 1997, **36**, 1808-1832.
38. E. Johnson, S. Keinan, P. Mori-Sanchez, J. Contreras-Garcia, A. J. Cohen and W. Yang, *J. Am. Chem. Soc.*, 2010, **132**, 6498-6506.
39. J. Contreras-Garcia, E. R. Johnson, S. Keinan, R. Chaudret, J. P. Piquemal, D. N. Beratan and W. Yang, *J. Chem. Theor. Comput.*, 2011, **7**, 625-632.
40. Y. Minenkov, A. Singstad, G. Occhipinti and V. R. Jensen, *Dalton Trans.*, 2012, **41**, 5526-5541.
41. M. Bühl, C. Reimann, D. A. Pantazis, T. Bredow and F. Neese, *J. Chem. Theory Comput.*, 2008, **4**, 1449-1459.
42. K. K. Pandey, S. K. Patidar, P. Patidar, R. Vishwakarma and P. K. Bariya, *Z. Anorg. Allg. Chem.*, 2014, **640**, 370-379.
43. J. Rezac and P. Hobza, *J. Chem. Theory Comput.*, 2013, **9**, 2151−2155.
44. W. Hujo and S. Grimme, *Phys. Chem. Chem. Phys.*, 2011, **13**, 13942-13950.
45. O. A. Vydrov and T. Van Voorhis, *J. Chem. Phys.*, 2010, **133**, 44103-44103.
46. A. Klamt, *J. Phys. Chem.*, 1995, **99**, 2224-2235.
47. A. Klamt and V. Jonas, *J. Chem. Phys.*, 1996, **105**, 9972-9981.
48. A. Klamt and G. Schueuermann, *J. Chem. Soc., Perkin Trans. 2*, 1993, 799-805.
49. F. B. van Duijneveldt, J. G. C. M. van Duijneveldt-van de Rijdt and J. H. van Lenthe, *Chem. Rev.*, 1994, **94**, 1873-1885.
50. Y. J. Jeon, S.-Y. Kim, Y. H. Ko, S. Sakamoto, K. Yamaguchi and K. Kim, *Org. Biomol. Chem.*, 2005, **3**, 2122-2125.
51. W. Iali, P. Petrovic, M. Pfeffer, S. Grimme and J.-P. Djukic, *Dalton Trans.*, 2012, **41**, 12233-12243.
52. E. Freire, O. Mayorga and M. Straume, *Anal. Chem.*, 1990, **62**, 950A-959A.

53. A. Valazquez-Campoy and E. Freire, *Biophys. Chem.*, 2005, **115**, 115-124.
54. R. G. Khalifah, F. Zhang, J. S. Parr and E. S. Rowe, *Biochemistry*, 1993, **32**, 3058-3066.
55. C. C. Pye, T. Ziegler, E. van Lenthe and J. N. Louwen, *Can. J. Chem.*, 2009, **87**, 790-797.
56. F. Biedermann, V. D. Uzunova, O. A. Scherman, W. M. Nau and A. de Simone, *J. Am. Chem. Soc.*, 2012, **134**, 15318-15323.
57. C. N. Nguyen, T. K. Young and M. K. Gilson, *J. Chem. Phys.*, 2012, **137**, 044101.
58. N. S. Venkataramanan, S. Ambigapathy, H. Mizuseki and Y. Kawazoe, *J. Phys. Chem. B*, 2012, **116**, 14029-14039.
59. A. Suvitha, N. S. Venkataramanan, H. Mizuseki, Y. Kawazoe and N. Ohuchi, *J. Inclusion Phenom. Macrocyclic Chem.*, 2010, **66**, 213-218.
60. H. Kruse, L. Goerigk and S. Grimme, *J. Org. Chem.*, 2012, **77**, 10824-10834.
61. S. Grimme, *J. Phys. Chem. A*, 2005, **109**, 3067-3077.
62. S. Grimme, *Angew. Chem. Int. Ed.*, 2006, **45**, 4460-4464.
63. S. Grimme, *Chem. Eur. J.*, 2012, **18**, 9955-9964.
64. T. A. K. Al-Allaf, L. J. Rashan, G. Ketler, H.-H. Fiebig and A. H. Al-Dujaili, *Appl. Organomet. Chem.*, 2009, **23**, 173-178.
65. D. Bardelang, K. A. Udachin, D. M. Leek, J. C. Margeson, G. Chan, C. I. Ratcliffe and J. A. Ripmeester, *Cryst. Growth Des.*, 2011, **11**, 5598-5614.
66. C. F. Guerra, J. G. Snijders, G. te Velde and E. J. Baerends, *Theor. Chem. Acc.*, 1998, **99**, 391-403.
67. E. J. Baerends, T. Ziegler, J. Autschbach, D. Bashford, A. Bérces, F. M. Bickelhaupt, C. Bo, P. M. Boerrigter, L. Cavallo, D. P. Chong, L. Deng, R. M. Dickson, D. E. Ellis, M. van Faassen, L. Fan, T. H. Fischer, C. F. Guerra, A. Ghysels, A. Giammona, S. J. A. van Gisbergen, A. W. Götz, J. A. Groeneveld, O. V. Gritsenko, M. Grüning, S. Gusarov, F. E. Harris, P. van den Hoek, C. R. Jacob, H. Jacobsen, L. Jensen, J. W. Kaminski, G. van Kessel, F. Kootstra, A. Kovalenko, M. V. Krykunov, E. van Lenthe, D. A. McCormack, A. Michalak, M. Mitoraj, J. Neugebauer, V. P. Nicu, L. Noodleman, V. P. Osinga, S. Patchkovskii, P. H. T. Philipsen, D. Post, C. C. Pye, W. Ravenek, J. I. Rodríguez, P. Ros, P. R. T. Schipper, G. Schreckenbach, J. S. Seldenthuis, M. Seth, J. G. Snijders, M. Solà, M. Swart, D. Swerhone, G. te Velde, P. Vernooijs, L. Versluis, L. Visscher, O. Visser, F. Wang, T. A. Wesolowski, E. M. van Wezenbeek, G. Wiesenekker, S. K. Wolff, T. K. Woo and A. L. Yakovlev, *Amsterdam Density Functional*, 2012, SCM, Theoretical Chemistry, Vrije Universiteit, Amsterdam, The Netherlands.
68. E. D. Glendening, J. K. Badenhoop, A. E. Reed, J. E. Carpenter, J. A. Bohmann, C. M. Morales and F. Weinhold, in *NBO 5.0*, Theoretical Chemistry Institute, University of Wisconsin, Madison, USA, 2001.
69. M. J. Frisch, G. W. Trucks, H. B. Schlegel, G. E. Scuseria, M. A. Robb, J. R. Cheeseman, G. Scalmani, V. Barone, B. Mennucci, G. A. Petersson, H. Nakatsuji, M. Caricato, X. Li, H. P. Hratchian, A. F. Izmaylov, J. Bloino, G. Zheng, J. L. Sonnenberg, M. Hada, M. Ehara, K. Toyota, R. Fukuda, J. Hasegawa, M. Ishida, T. Nakajima, Y. Honda, O. Kitao, H. Nakai, T. Vreven, J. J. A. Montgomery, J. E. Peralta, F. Ogliaro, M. Bearpark, J. J. Heyd, E. Brothers, K. N. Kudin, V. N. Staroverov, R. Kobayashi, J. Normand, K. Raghavachari, A. Rendell, J. C. Burant, S. S. Iyengar, J. Tomasi, M. Cossi, N. Rega, J. M. Millam, M. Klene, J. E. Knox, J. B. Cross, V. Bakken, C. Adamo, J. Jaramillo, R. Gomperts, R. E. Stratmann, O. Yazyev, A. J. Austin, R. Cammi, C. Pomelli, J. W. Ochterski, R. L. Martin, K. Morokuma, V. G. Zakrzewski, G. A. Voth, P. Salvador, J. J. Dannenberg, S. Dapprich, A. D. Daniels, Ö. Farkas, J. B. Foresman, J. V. Ortiz, J. Cioslowski and D. J. Fox, Gaussian, Inc., Wallingford, CT, 2010.
70. C. Møller and M. Plesset, *Phys. Rev. A*, 1934, **46**, 618-622.
71. J. Čižek, *J. Chem. Phys.*, 1966, **45**, 4256-4266.
72. J. Čižek and J. Paldus, *Int. J. Quantum Chem.*, 1971, **5**, 359-379.
73. J. Paldus, J. Čižek and I. Shavitt, *Phys. Rev. A,* 1972, **5**, 50-67.
74. M. Musiał and R. J. Bartlett, *Rev. Mod. Phys.*, 2007, **79**, 291-352.
75. K. Raghavachari, G. W. Trucks, J. A. Pople and M. Head-Gordon, *Chem. Phys. Lett.*, 1989, **157**, 479-483.
76. I. D. Mackie and G. A. di Labio, *J. Chem. Phys.*, 2011, **135**, 134318.
77. S. F. Boys and F.Bernardi, *Mol. Phys.*, 1970, **19**, 553-566.
78. D. E. Woon and T. H. Dunning Jr., *J. Chem. Phys.*, 1993, **98**, 1358-1371.
79. R. A. Kendall, T. H. Dunning Jr. and R. J. Harrison, *J. Chem. Phys.*, 1992, **96**, 6796-6806.
80. M. O. Sinnokrot and C. D. Sherrill, *J. Phys. Chem. A*, 2004, **108**, 10200-10207.